Modulation of Gramicidin Channel Structure and Function by the Aliphatic "Spacer" Residues 10, 12, and 14 between the Tryptophans†

Anthony R. Jude,‡ Denise V. Greathouse,‡ Roger E. Koeppe II,*,‡ Lyndon L. Providence,§ and Olaf S. Andersen§

Department of Chemistry and Biochemistry, University of Arkansas, Fayetteville, Arkansas 72701, and Department of Physiology and Biophysics, Cornell University Medical College, New York, New York 10021

Received August 24, 1998; Revised Manuscript Received November 16, 1998

ABSTRACT: In the linear gramicidins, the four aromatic residues at positions 9, 11, 13, and 15 are well-known to be important for the structure and function of membrane-spanning gramicidin channels. To investigate whether the "spacer" residues between the tryptophans in gramicidin A (gA) are important for channel structure and function, D-Leu-10, -12. and -14 of gA were replaced by Ala, Val, or Ile. (For practical reasons, the Ile substitutions were introduced into the enantiomeric gramicidin A^-, gA^-.) Circular dichroism spectra of [D-$Ala^{10,12,14}$]gA, [D-$Val^{10,12,14}$]gA, or [$Ile^{10,12,14}$]gA^- incorporated into sodium dodecyl sulfate micelles or 1,2-dimyristoyl-*sn*-glycero-3-phosphocholine vesicles differ from the spectrum of the native [D-$Leu^{10,12,14}$]gA. All the analogue spectra display reduced ellipticity at both 218 and 235 nm, indicating the presence of double-stranded conformers with the Ala analogue spectra showing the largest departure from the native gA spectra. Size-exclusion chromatograms of the Val and Ile analogues show both monomer and dimer peaks, accompanied by peak broadening; the chromatograms for the Ala analogue show broad, overlapping peaks and suggest the presence of higher oligomers and/or (rapidly) interconverting conformations. All three analogues form membrane-spanning channels, with the channel-forming potency of the Ala analogue being much less than that of gA or the other analogues. In 1.0 M CsCl, the conductance of each analogue channel is ∼25% less than that of [D-$Leu^{10,12,14}$]gA channels. The lifetimes of the analogue channels also are less than of [D-$Leu^{10,12,14}$]gA channels, with the largest (8-fold) reduction being for [D-$Ala^{10,12,14}$]gA channels. Hybrid channel experiments show that the $\beta^{6.3}$-helical backbone folding pattern is retained in the channel-forming subunits and that the substitutions primarily influence ion entry. Both the bulk and the stereochemistry of the aliphatic residues between the tryptophans of gA are important for channel structure and function.

In membrane proteins of known tertiary structure, the aromatic amino acids Trp and Tyr cluster at or near the membrane/water interface (*1*−*5*). Trp, for example, has an amphipathic indole side chain, which seeks not only a nonpolar environment for its six-membered ring but also a polar environment in which the N−H of the five-membered ring can form a hydrogen bond to a suitable acceptor. In a phospholipid membrane, therefore, Trp will endeavor to position its six-membered ring within the hydrophobic membrane interior formed by the lipid hydrocarbon chains, while leaving the N−H exposed at the membrane surface. This principle for the organization of Trp in membranes also is seen in gramicidin (gA[1]) channels, in which each end of a dimeric channel presents 4 Trp side chains (at positions 9, 11, 13, and 15) at the membrane/water interface (Table 1; *6*−*12*). If any one of the Trps is replaced by Phe, the single-channel conductance for Na^+ or Cs^+ ions decreases, by 25−60% depending on the position that is modified (*7*, *13*). Further, the Trps anchor each gA monomer to the bilayer leaflet to which it initially is added (*6*), a result that suggests a more general structural and functional importance of having Trp residues at the membrane/solution interface. Finally, Trp → Phe substitutions change the conformational preference of bilayer-incorporated gramicidins by increasing the propensity to form (membrane-spanning) double-stranded dimers (*14*−*16*).

Separating the Trps in gA are three leucines (Figure 1). Surprisingly, in contrast to the recognized importance of the tryptophans (*7*, *12*, *15*−*26*), there have been no studies on the role of these "spacer" Leu residues between the Trps. We therefore examined the effects of substituting the reference $Leu^{10,12,14}$ by the semiconservative $Ala^{10,12,14}$, $Val^{10,12,14}$, or $Ile^{10,12,14}$ (Table 1) and found large differences in the properties of gA channels having different spacer residues. The results suggest that neighboring residue effects on Trp side chains at the membrane/water interface are important for gramicidin channel function. Similar effects are likely to be important for membrane proteins generally.

† This work was supported in part by Grants GM21342 and GM34968 from the NIH.

‡ University of Arkansas.

§ Cornell University Medical College.

[1] List of Abbreviations: gA, gramicidin A; gA^-, enantiomer of gA; CD, circular dichroism; DLPC, dilauroylphosphatidylcholine; DMF, dimethylformamide; DMPC, dimyristoylphosphatidylcholine; DOPC, dioleoylphosphatidylcholine; DPhPC, diphytanoylphosphatidylcholine; DS, double-stranded; EtOH, ethanol; HBTU, *O*-benzotriazol-1-yl-*N*,*N*,*N*′,*N*′-tetramethyluronium hexafluorophosphate; HOBT, 1-hydroxybenzotriazole; LH, left-handed; MeOH, methanol; RH, right-handed; SDS, sodium dodecyl sulfate; SEC, size-exclusion (high-performance liquid) chromatography; SS, single-stranded; THF, tetrahydrofuran.

10.1021/bi982043m CCC: $18.00
Published on Web 12/29/1998

Table 1: Sequences of Gramicidin A Analogues[a]

Analogue (Abbr.)	Sequence (chirality)
	(L D L D L D L)
Gramicidin A (gA)	R-Trp-Leu-Trp-Leu-Trp-Leu-Trp-$NHCH_2CH_2OH$
	9 10 11 12 13 14 15
[D-$Ala^{10,12,14}$]gA	R-Trp-**Ala**-Trp-**Ala**-Trp-**Ala**-Trp-$NHCH_2CH_2OH$
[D-$Val^{10,12,14}$]gA	R-Trp-**Val**-Trp-**Val**-Trp-**Val**-Trp-$NHCH_2CH_2OH$
[$Ile^{10,12,14}$]gA*	R*-Trp-**Ile**- Trp-**Ile**- Trp-**Ile**- Trp-$NHCH_2CH_2OH$

[a] R = HCO-L-Val^1-Gly^2-L-Ala^3-D-Leu^4-L-Ala^5-D-Val^6-L-Val^7-D-Val^8. The designation [$Ile^{10,12,14}$]gA* indicates that the entantiomer ([L-$Ile^{10,12,14}$]gA^-) of the listed sequence was synthesized, and for ease of comparison with the other analogues, the CD spectra of the enantiomer were mathematically inverted prior to printing Figures 2 and 3.

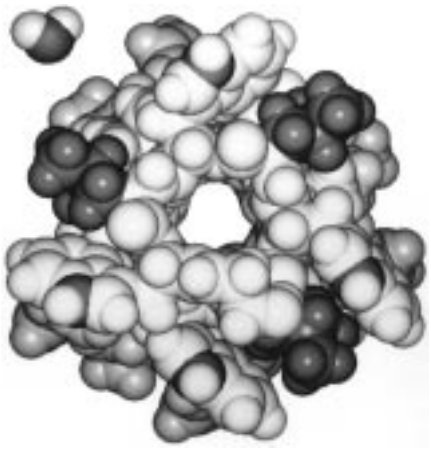

FIGURE 1: End view of a space-filling model of [D-$Leu^{10,12,14}$]gA. The side chains of Leu 10, 12, and 14 are highlighted in dark, as are the indole nitrogen atoms of Trp 9, 11, 13, and 15. Coordinates are from Arseniev (*70*), as modified in ref *71*. The indicated leucine residues were substituted to give the sequences listed in Table 1. A water molecule is shown on the same scale.

MATERIAL AND METHODS

Materials. Formyl-L-Val and formyl-D-Val were synthesized as in ref *27*. Fmoc amino acids and Fmoc-L-Trp resin were from Bachem (Philadelphia, PA), Peninsula Labs (Belmont, CA), and Advanced Chemtech (Louisville, KY). HBTU, piperidine, and *N*-methylmorpholine were from Rainin Instrument Co. (Woburn, MA). DMF, EtOH (anhydrous), and ethanolamine were from Aldrich Chemical Co. (Milwaukee, WI); the latter was distilled in vacuo (*28*). DMPC and DPhPC were from Avanti Polar Lipids (Alabaster, AL). MeOH, high purity for SEC and CD, was from Baxter Diagnostics Inc. (McGaw Park, IL). All other chemicals for CD and SEC were as in ref *29* and, for single-channel measurements, as in ref *28*.

Peptide Synthesis. [D-$Ala^{10,12,14}$]gA and [D-$Val^{10,12,14}$]gA were synthesized using Fmoc-L-Trp resin, which was deprotected and extended using a Rainin model SP3 peptide synthesizer (Emeryville, CA) to produce the desired sequence using Fmoc amino acid precursors, followed by formyl-L-Val at the last step. Each residue was coupled in sequence using HOBT chemistry, which consists of deprotecting the N-terminus of the growing chain with piperidine, activating the subsequent residue using HBTU, yielding an HOBT-ester intermediate, and coupling at the N-terminus (*30*). The peptides were cleaved from the resins using 50% ethanolamine in DMF at 55 °C, as described previously (*7*). Purification was done by passing the cleaved peptide through two separate Zorbax C8 columns from DuPont Co. (Wilmington, DE; see ref *27*). Prior to the reversed-phase chromatography, it was necessary to remove low-molecular weight impurities from [D-$Ala^{10,12,14}$]gA by chromatographing samples in methanol over a Sephadex LH-20 column from Pharmacia (purchased through Sigma Chemical Co., St. Louis, MO).

The enantiomer of [D-$Ile^{10,12,14}$]gA, [$Ile^{10,12,14}$]gA^-, was synthesized, using the HOBT chemistry described above. Chiral interactions between the phospholipid backbone and the host bilayer are not important determinants of gramicidin channel structure or function because the characteristics of channels formed by gramicidin A and its enantiomer (gA^-) are indistinguishable from each other (*31*), regardless of lipid chirality (*32*). Fmoc-D-Trp resin and formyl-D-Val were used for positions 15 and 1, respectively, of [$Ile^{10,12,14}$]gA^-, with alternating L- and D-Fmoc amino acids for the remainder of the sequence.

CD Spectroscopy and SEC. Samples for CD spectroscopy and SEC in MeOH and EtOH were prepared by resuspending 0.05 μmol (100 μg) of dry peptide in 100 μL of solvent. Final sample concentrations were determined by measuring A_{280} and using $\epsilon_{280} = 21\,000\ M^{-1}\ cm^{-1}$ (*33*). Samples for CD spectroscopy and SEC in DMPC and SDS were prepared as described previously (*29*) using 0.05 μmol of gA analogue plus either 1.4 μmol of DMPC (1:28 gramicidin:lipid ratio) or 2.5 μmol of SDS (1:50 gramicidin:SDS ratio) in a final volume of 500 μL of H_2O. Briefly, dry gramicidin/lipid (or gramicidin/SDS) films were prepared by evaporating all traces of solvent from methanol/chloroform solutions, resuspending in N_2-flushed H_2O, and sonicating at 55 °C to produce small vesicles (or micelles).

Except in very short lipids (*29*), or very long lipids (*34*), the structure and CD spectrum of gA in phospholipid membranes and in SDS are remarkably constant over a large range of peptide/lipid ratios. In DOPC, the structure of gA is invariant within the bilayer up to a gramicidin/lipid ratio ≈1:15 (with an inverted lipid phase and phase separation occurring at higher ratios (*35*)). In DLPC, X-ray scattering with momentum transfer in the plane of the membrane shows that gA at 1:10 behaves as freely diffusing (nonaggregated) dimers (*36*, *37*). In DMPC at 1:8, solid-state NMR shows that these dimers are SS and RH (*9*) and rotate rapidly about the long molecular axis (*38*). In DMPC or in SDS, the CD spectrum of gA is essentially invariant over a range from 1:10 to at least 1:330 (*39*, *40*). Therefore, gramicidin/lipid ratios of 1:50−1:25 are appropriate and convenient for CD and SEC and are well within the invariant range for gA structure; the results should be relevant for understanding membrane-spanning channels studied by single-channel methods.

CD spectra were recorded at 22−24 °C using a Jasco J-710 circular dichroism spectrometer with a 0.1 cm path length cell. The spectra were recorded with 1.0 nm bandwidth, 0.2 nm step resolution, and 20 or 50 nm/min scan speed. Six or twelve scans were averaged to give the spectra shown in this article. To facilitate comparison with the spectra obtained with gA and the other analogues, the spectra of [$Ile^{10,12,14}$]gA^-

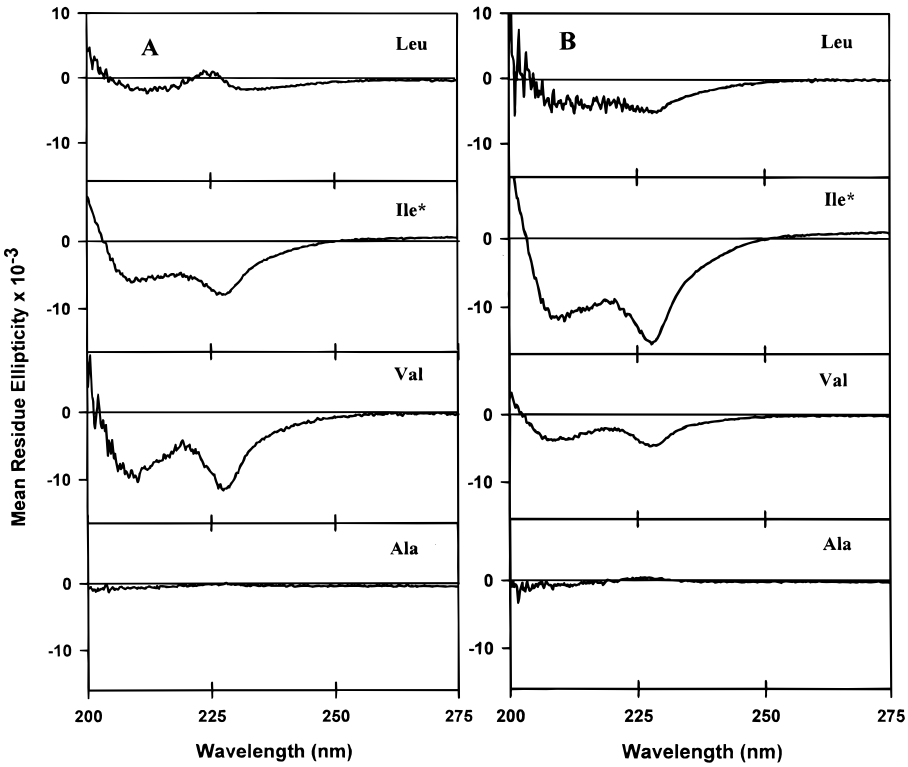

FIGURE 2: CD spectra of [D-Leu^{10,12,14}]gA, [Ile^{10,12,14}]gA*, [D-Val^{10,12,14}]gA, or [D-Ala^{10,12,14}]gA at 22−24 °C in MeOH (A) or EtOH (B). The labels indicate the identity of the amino acid at positions 10, 12, and 14. (The spectra for [Ile^{10,12,14}]gA$^-$ were inverted and labeled Ile* for comparison with the gA$^+$ series of analogues.)

were inverted; we label the inverted spectra with the designation [Ile^{10,12,14}]gA*.

The fractions of DS and SS conformers in organic solvents or lipid suspensions were determined by SEC at room temperature as described in ref *41* using an Ultrastyragel 1000 Å column (Waters, Inc., Milford, MA) with a THF mobile phase at a flow rate of 1.0 mL/min.

Electrophysiology. Single-channel measurements were done in planar bilayers formed from DPhPC in *n*-decane (2−3% w/v) at 25 ± 1 °C, using the bilayer punch method (*42*). Sample preparation was as described by Mattice et al. (*28*). Gramicidins were added in amounts necessary to produce ∼1 channel event/s. Data analysis was as described in refs *13* and *43*.

RESULTS

Several methods were used to assess the effects of Leu^{10,12,14} substitutions on gramicidin structure and function.

CD Spectroscopy. [D-Leu^{10,12,14}]gA itself is known to adopt different types of conformations in different solvent environments. In MeOH (Figure 2A), the native [D-Leu^{10,12,14}]gA is predominantly unstructured and characterized by a CD spectrum with negative minima near 210 and 235 nm and positive ellipticity below 205 nm (*44*). In EtOH (Figure 2B), [D-Leu^{10,12,14}]gA adopts a mixture of several interconverting DS conformations (*45*) that give a CD spectrum characterized by positive ellipticity below 205 nm and negative ellipticity from 205 to 250 nm (Figure 2B).

The CD spectra of [Ile^{10,12,14}]gA*, [D-Val^{10,12,14}]gA, and [D-Ala^{10,12,14}]gA differ qualitatively from those of native [D-Leu^{10,12,14}]gA in both MeOH and EtOH (Figure 2). The spectra of [D-Ala^{10,12,14}]gA show no definite positive or negative ellipticity in either solvent. The differences relate to both the peptide sequence and the particular environment (see below). By comparison with the CD spectra in phospholipid vesicles or detergent micelles (Figure 3), these spectra show that neither [D-Leu^{10,12,14}]gA nor the Leu^{10,12,14}-substituted analogues adopt a channel conformation in MeOH or EtOH.

In phospholipid bilayers, such as DMPC vesicles, [D-Leu^{10,12,14}]gA adopts a RH $\beta^{6.3}$ SS channel conformation whose CD spectrum is characterized by positive maxima near 218 and 235 nm, a minimum at 230 nm, and negative ellipticity below 208 nm (Figure 3A; see also refs *29*, *46*, and *47*). The CD spectrum of [Ile^{10,12,14}]gA* in DMPC vesicles (Figure 3A) exhibits a maximum at ∼218 nm, a negative minimum at ∼229 nm, and a positive ellipticity near 200 nm. The maximum at ∼218 nm is characteristic of the RH SS conformation (cf. the spectrum for [D-Leu^{10,12,14}]-gA), whereas the latter two features are characteristic of DS conformations. The CD spectrum of [D-Val^{10,12,14}]gA in DMPC vesicles (Figure 3A) is similar to that of [Ile^{10,12,14}]-gA*, again suggesting the presence of both SS and DS conformations.

As was the case in MeOH and EtOH, the CD spectrum of [D-Ala^{10,12,14}]gA in DMPC vesicles (Figure 3A) is very different from those of [D-Leu^{10,12,14}]gA, [D-Val^{10,12,14}]gA, or [Ile^{10,12,14}]gA*. The [D-Ala^{10,12,14}]gA spectrum displays no distinct maximum or minimum but rather a broad positive ellipticity between ∼215 and 240 nm and a negative ellipticity at 200 nm. By comparison with the other spectra in Figure 3A and those in ref *29*, these features are consistent with the presence of a (RH) SS conformation; but the absence of distinct maxima or minima is unusual for lipid-incorporated gramicidin (see discussion).

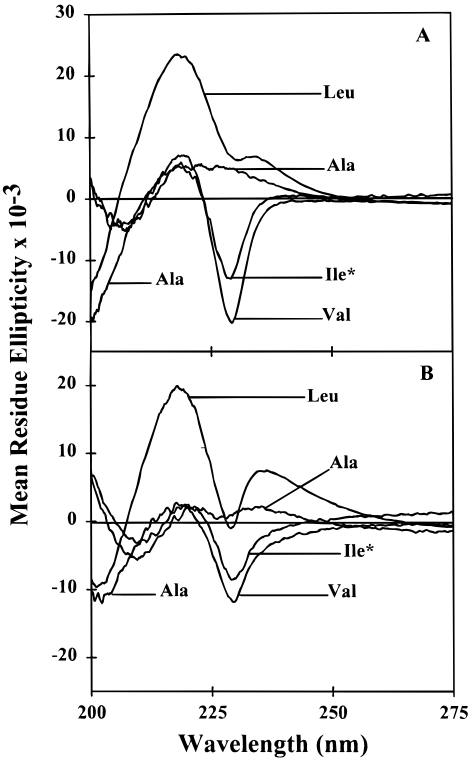

FIGURE 3: CD spectra of [D-Leu^{10,12,14}]gA, [Ile^{10,12,14}]gA*, [D-Val^{10,12,14}]gA, or [D-Ala^{10,12,14}]gA at 22−24 °C in aqueous DMPC at 1:28 gramicidin:lipid ratio (A) or SDS at 1:50 gramicidin:SDS ratio (B). (The spectra of [Ile^{10,12,14}]gA$^-$ were inverted and designated Ile* for comparison with gA$^+$ series.)

The CD spectra of [D-Leu^{10,12,14}]gA, [Ile^{10,12,14}]gA,* and [D-Val^{10,12,14}]gA change little when the environment is switched from DMPC vesicles to SDS micelles (Figure 3B). The spectrum of [D-Leu^{10,12,14}]gA shows more pronounced negative ellipticity at ∼229 nm, but there is variability from preparation to preparation (see also ref *47* and *39*). The spectra of [Ile^{10,12,14}]gA* and [D-Val^{10,12,14}]gA show slightly decreased magnitudes of the positive and negative ellipticities at ∼218 and ∼229 nm, respectively, and a more pronounced positive ellipticity at 200 nm (Figure 3B). The spectrum of [D-Ala^{10,12,14}]gA changes somewhat when going from DMPC vesicles to SDS micelles. The absolute ellipticity remains low, but there are two maxima at ∼235 and ∼218 nm, which are separated by a minimum at ∼225 nm, and a negative ellipticity below ∼215 nm. These features are qualitatively similar to those of the [D-Leu^{10,12,14}]gA spectrum and suggest that for [D-Ala^{10,12,14}]gA the RH SS conformation is relatively favored in SDS micelles, as compared to DMPC vesicles.

Although the spectra in Figure 3A,B are remarkably similar (given the lipid/detergent difference), we wondered whether the spectrum of [D-Ala^{10,12,14}]gA was influenced by the presence of the sodium ions from the SDS. For native [D-Leu^{10,12,14}], there are dramatic conformational changes when Cs^+ ions are added to solutions of gA in MeOH or EtOH (*47*−*51*) but not when Cs^+ is added to gA channels in DMPC (*47*). We confirm this result for gA in DMPC in Figure 4A and show that 0.5 M Cs^+ similarly has no effect on [D-Ala^{10,12,14}]gA in DMPC (Figure 4B). Whether the sample is gA (in the channel conformation) or [D-Ala^{10,12,14}]-gA (only partially in the channel conformation), Cs^+ cannot alter significantly the conformational mixture (Figure 4).

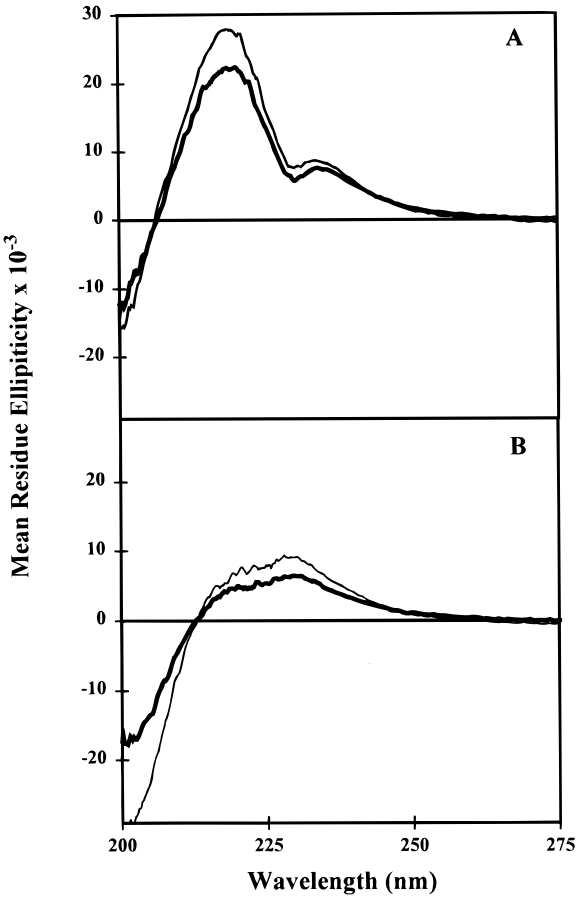

FIGURE 4: CD spectra of (A) native [D-Leu^{10,12,14}]gA and (B) [D-Ala^{10,12,14}]gA at 1:28 in hydrated DMPC, with 0.5 M Cs^+ (—) and without salt (−).

Size Exclusion Chromatography. The CD spectra show that substantial fractions of the Leu^{10,12,14}-substituted gA analogues occur as DS conformers—even in lipid bilayers or bilayerlike environments. In the absence of well-defined reference spectra for the different components, however, one needs alternative methods to characterize the distribution between SS and DS conformers. We examined this question using SEC. In SEC, a small volume of the appropriate gA dissolved in an organic solvent, or incorporated into phospholipid vesicles, is injected into flowing THF, which dilutes (removes) the solvent and dissolves (or disrupts) the bilayer or micelle structure (*41*). Moreover, the THF "quenches" whatever structure the gramicidin may be in because THF does not participate in hydrogen bond formation with the peptide backbone. Dissolution of the gA−phospholipid assembly will lead to dissociation of the six intermolecular hydrogen bonds that stabilize the SS dimers (the channel conformation) so SS dimers will elute as monomers. Any DS conformations, which are stabilized by 28 intermolecular hydrogen bonds (*52*), remain intact and elute as dimers (*41*).

Figure 5 shows SEC results for the native [D-Leu^{10,12,14}]-gA and the Leu^{10,12,14}-substituted gA analogues in EtOH and MeOH. The elution profile of [D-Leu^{10,12,14}]gA in MeOH (Figure 5A) shows a dimer peak, with an elution time of 8.7 min and a relative peak area of about 0.1, and a monomer peak, with an elution time of 9.2 min and a relative peak area of about 0.9. On the basis of CD spectroscopy (Figure 2), these gA monomers in MeOH represent a mixture of unfolded or unstructured conformations and neither a "chan-

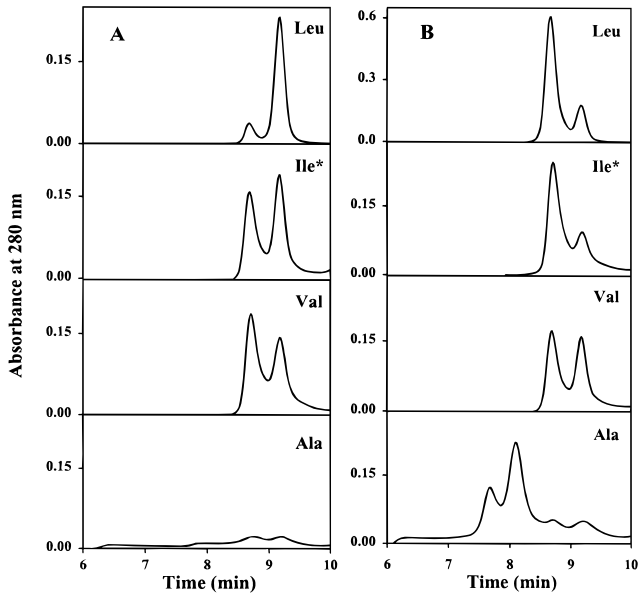

FIGURE 5: SEC elution profiles for [D-Leu^{10,12,14}]gA, [Ile^{10,12,14}]gA$^-$, [D-Val^{10,12,14}]gA, and [D-Ala^{10,12,14}]gA dissolved in MeOH (A) or EtOH (B). A 10 μL sample of a 1 mg/mL solution of each peptide in the indicated solvent was injected into THF flowing at 1.0 mL/min. Each profile is labeled by the identity of the amino acid at positions 10, 12, and 14.

nel" conformation nor the DS conformation that crystallizes (*53*). The comparable experiment with [D-Leu^{10,12,14}]gA in EtOH (Figure 5B) again shows both dimer and monomer peaks but with the relative areas being reversed—to 0.8 and 0.2, respectively. These elution profiles are in good agreement with previously published data, which show that the DS dimer component elutes about 0.5 min prior to the monomer component (*41*). The differences between the elution profiles in EtOH and MeOH confirm the solvent dependence of the structural preference of [D-Leu^{10,12,14}]gA.

[Ile^{10,12,14}]gA$^-$ and [D-Val^{10,12,14}]gA likewise show pronounced dimer and monomer components in both MeOH and EtOH (Figure 5). In comparison to [Leu^{10,12,14}]gA, the chromatograms for [Ile^{10,12,14}]gA$^-$ and [D-Val^{10,12,14}]gA show more pronounced dimer peaks in MeOH. Interestingly, however, the two analogues show different SS/DS shifts when going from MeOH to EtOH.

The chromatograms of [D-Ala^{10,12,14}]gA, whether in MeOH or EtOH, show the largest changes from gA. In MeOH (Figure 5A), [D-Ala^{10,12,14}]gA begins to elute at approximately 6.2 min and has an elution profile that has several broad, overlapping peaks. According to standard chromatography theory, the first two peaks, at ~6.4 and ~7.8 min, correspond to higher order aggregates. The peaks at 8.7 and 9.2 min correspond to the DS and SS components described above. The broad and overlapping peaks complicate attempts to determine the relative peak areas, which were not evaluated quantitatively. The elution profile of [D-Ala^{10,12,14}]gA in EtOH (Figure 5B), shows an even more pronounced tendency toward aggregation into higher oligomers. Again, [D-Ala^{10,12,14}]gA begins to elute at approximately 6.2 min and displays (at least) four peaks. The well-defined early peaks, at 7.7 and 8.1 min, have relative peak areas of 0.2 and 0.6, respectively. The last two peaks, which have elution times corresponding to the dimer and monomer, again have peak areas that are difficult to determine.

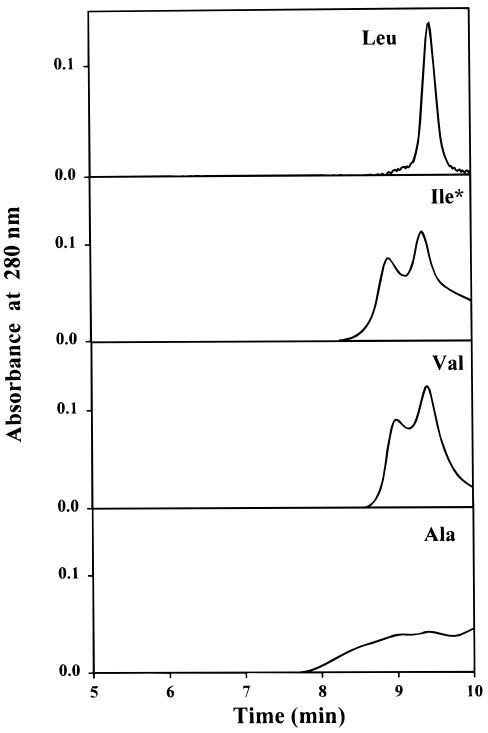

FIGURE 6: SEC elution profiles of [D-Leu^{10,12,14}]gA, [Ile^{10,12,14}]gA$^-$, [D-Val^{10,12,14}]gA, and [D-Ala^{10,12,14}]gA in phospholipid membranes. A 5 μL volume of a 1:28 analogue:DMPC aqueous suspension ratio was injected into THF flowing at 1.0 mL/min. Each profile is labeled by the identity of the amino acid at positions 10, 12, and 14.

Figure 6 shows elution profiles for [D-Leu^{10,12,14}]gA, [Ile^{10,12,14}]gA$^-$, [D-Val^{10,12,14}]gA, and [D-Ala^{10,12,14}]gA after incorporation into DMPC vesicles. The profile for [D-Leu^{10,12,14}]gA shows no dimer peak, only a monomer peak that derives from the channel conformation with an elution time of 9.5 min (relative area 1.0; Figure 6). (DS conformers would be expected to elute approximately 0.5 min prior to the monomer peak (*54*); see also Figure 5.) The elution profile for [Ile^{10,12,14}]gA$^-$ shows a dimer peak at 9.0 min (relative area ~0.4) along with a monomer peak at 9.4 min (relative area ~0.6). On the basis of the CD spectra and the observation of channel activity (see below), a significant fraction, if not all, of the monomer peak results from membrane-spanning SS $\beta^{6.3}$-helical dimers, as established previously for [D-Leu^{10,12,14}]gA (*54*). The elution profile for [D-Val^{10,12,14}]gA is similar to that for [Ile^{10,12,14}]gA$^-$, again displaying peaks at 8.9 and 9.3 min, with relative peak areas of ~0.4 and ~0.6, respectively. The smaller difference between the peak retention times for the DMPC-incorporated analogues, and the peak broadening seen with these analogues as compared to the results in MeOH and EtOH, may arise from the presence of the lipids in the mixture or, possibly, from exchange between SS and DS conformers during the chromatography. In any case, the chromatograms and the CD spectra show that significant fractions of both [Ile^{10,12,14}]gA$^-$ and [D-Val^{10,12,14}]gA occur as DS conformers in DMPC vesicles; there is also a population of monomeric SS conformers, which we attribute to membrane-spanning SS dimers—similar to the case for the native [Leu^{10,12,14}]gA.

[D-Ala^{10,12,14}]gA once again exhibits unusual characteristics. The SEC elution profile consists of a broad peak, or many overlapping peaks without distinguishable minima, and

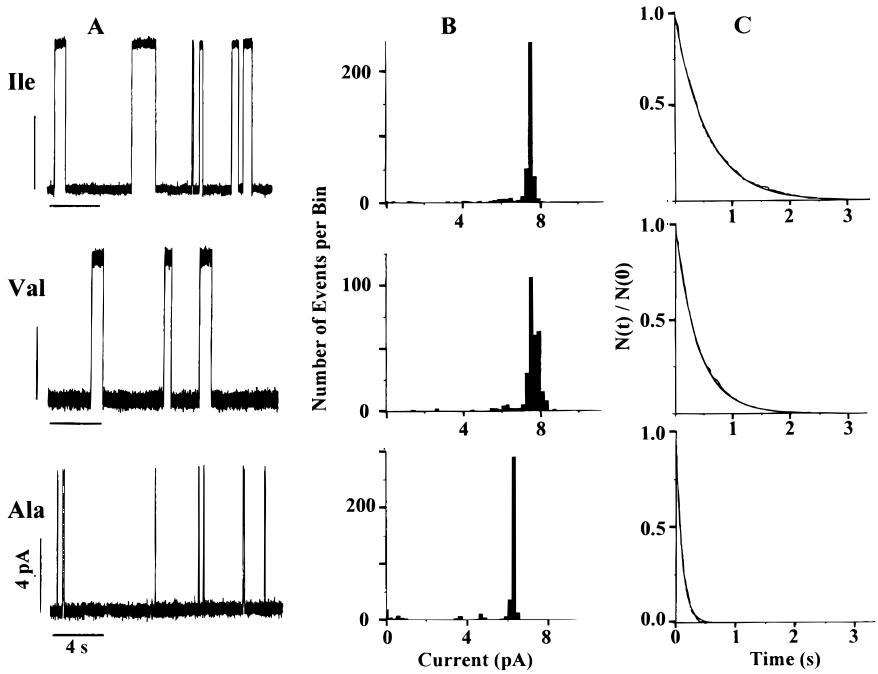

FIGURE 7: Single-channel current traces (A), current transition amplitude histograms (B), and lifetime distributions (C) for [Ile^{10,12,14}]gA$^-$, [D-Val^{10,12,14}]gA, and [D-Ala^{10,12,14}]gA channels. Current traces are shown using identical current and time scales with channel appearances occurring upward. The calibration bars denote 4 pA (vertically) and 4 s (horizontally). The average single-channel conductances are listed in Table 2. The % of current transitions in the major peak varies between 90% for [Ile^{10,12,14}]gA$^-$ and 93% for [D-Val^{10,12,14}]gA. The lifetime distributions are displayed as normalized survivor plots, and τ values are listed in Table 2. The continuous curves in part C show the fits of single-exponential distributions to the results. Conditions: 1.0 M CsCl; 200 mV; DPhPC/*n*-decane.

one cannot discern separate dimer and monomer peaks. The profile suggests the presence of multiple conformers and aggregation states and possibly interconvertions between SS and DS conformations (on the SEC time scale).

Single-Channel Characteristics. The CD spectra and SEC chromatograms suggest that all three Leu^{10,12,14}-substituted gA analogues form SS $\beta^{6.3}$-helices—even [D-Ala^{10,12,14}]gA. These analogues therefore should be able to form membrane-spanning channels in lipid bilayers. Given the conformational heterogeneity that is evident in the CD spectra and the SEC chromatograms, one might even have expected to observe several different channel types for a given analogue (but such is not the case).

The Leu^{10,12,14}-substituted gA analogues do indeed form channels. The pattern of channel appearances, as well as the functional characteristics of the analogue channels, were compared to those of native [D-Leu^{10,12,14}]gA channels. Figure 7 shows the single-channel current traces, current amplitude histograms, and lifetime distributions for the three analogues (1.0 M CsCl). Each of the traces (Figure 7A) displays a single population of current transitions, which suggests that each analogue forms only one conducting channel type. These channel events are seen only when the analogue in question is added to both sides of the bilayer (see Figure 8, below), which shows that the channels are formed by the transmembrane association of two nonconducting monomers. We therefore conclude, by analogy with previous results (*6*, *14*, *55*), that the channels we observe are SS $\beta^{6.3}$-helical dimers. The current transition amplitude histograms and lifetime distributions further confirm that each analogue forms only one type of conducting channel and that both the single-channel conductance and the average channel lifetime are altered by the sequence substitutions.

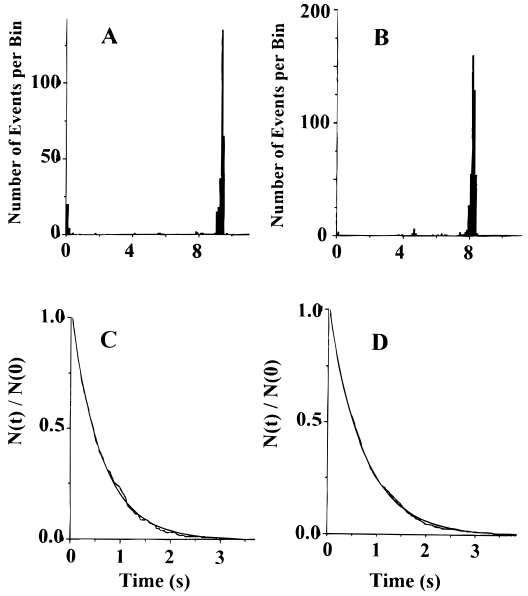

FIGURE 8: Hybrid channel experiment with gA$^-$ and [Ile^{10,12,14}]gA$^-$. (A) Histogram of single-channel currents observed across DPhPC after asymmetric addition of gA$^-$ and [Ile^{10,12,14}]gA$^-$, in which 271 of 310 events (87%) fall in the main peak at 9.25 $\pm$ 0.11 pA. (B) Histogram of single-channel currents observed when the voltage is changed from +100 to −100 mV across the same membrane used in experiment A; now 436 of 464 events (94%) fall in the main peak at 8.07 $\pm$ 0.12 pA. (C, D) Single-channel lifetime histograms corresponding to the events in panels A and B, respectively. The solid lines in C and D represent single-exponential fits in which τ is 606 ms for 243 events in C and 703 ms for 766 events in D.

The single-channel conductances (Figure 7B, Table 2) for [Ile^{10,12,14}]gA$^-$, [D-Val^{10,12,14}]gA, and [D-Ala^{10,12,14}]gA are 38, 38, and 31 pS, respectively. These values are 20−30% lower

Table 2: Single-Channel Conductances and Average Lifetimes of Channels Formed by Gramicidin A Analogues[a]

	g (pS)	τ (ms)	R_p
A. Homodimeric Channels			
[D-Leu^{10,12,14}]gA	47 ± 1	800	1
"spacer" analogue			
[Ile^{10,12,14}]gA$^-$	38 ± 1	550	0.1
[D-Val^{10,12,14}]gA	38 ± 1	400	0.1
[D-Ala^{10,12,14}]gA	31 ± 2	100	0.004
Trp → Phe analogue			
[Phe^{11}]gA	38 ± 2	1000	
B. Heterodimeric Channels			
analogue pair			
[Leu^{10,12,14}]gA$^-$/[Ile^{10,12,14}]gA$^-$	46 ± 1	610	
	40 ± 1	700	
[D-Leu^{10,12,14}]/[D-Val^{10,12,14}]gA	50 ± 2	620	
	40 ± 2	470	
[D-Leu^{10,12,14}]gA/[D-Ala^{10,12,14}]gA	45 ± 1	330	
	31 ± 1	280	

[a] [Leu^{10,12,14}]gA$^-$ and [Ile^{10,12,14}]gA$^-$ are the enantiomeric sequences of [D-Leu^{10,12,14}]gA and [D-Ile^{10,12,14}]gA. For the heterodimers, the channel properties depend on channel orientation (Figure 8). For each pair, the upper and lower entries refer to measurements where the [D-Leu^{10,12,14}]gA (or [Leu^{10,12,14}]gA$^-$) side of the channel is positive and negative, respectively. Conditions: 1.0 M CsCl; 200 mV; 25 °C; DPhPC/*n*-decane. Data for [Phe^{11}]gA are from refs *21* and *7*.

than that of native [D-Leu^{10,12,14}]gA channels (47 pS; e.g. ref *28* and surprisingly similar considering the differences seen in the CD spectra or the SEC chromatograms. The single-channel conductance is diminished whether the native Leu side chains at positions 10, 12, and 14 are mutated into smaller residues or residues that are geometrically altered at the β carbon. (For comparison, we also list in Table 2 the single-channel conductance and lifetime for a Trp → Phe substituted gA analogue, [Phe^{11}]gA, which forms channels that also have a ∼25% reduced conductance.) There is no discernible difference in the distribution of current transition amplitudes for the position-10, -12, and -14 analogues; the fraction of events in the main peak varies between 90% and 93%, which is comparable to what is seen with [D-Leu^{10,12,14}]-gA (*43*).

The lifetime distributions are shown in Figure 7C and summarized in Table 2. The histograms are well described by single exponential distributions, further confirming that each analogue forms a kinetically homogeneous population of channels. The average lifetime of each analogue channel is decreased relative to that of [D-Leu^{10,12,14}]gA channels (∼800 ms). [Ile^{10,12,14}]gA$^-$ and [D-Val^{10,12,14}]gA channels have lifetimes of 550 and 400 ms, respectively. A more dramatic change is observed with [D-Ala^{10,12,14}]gA channels, which exhibit an 8-fold decrease in lifetime to 100 ms.

As would be expected from the CD and SEC results, the analogues do not form channels as readily as the native [D-Leu^{10,12,14}]gA. We express this by their relative channel-forming potency (R_p), which denotes the inverse of the amount of analogue that one must add, relative to [D-Leu^{10,12,14}]-gA, to obtain a channel appearance rate of ∼1/s (Table 2). Consistent with the "abnormal" CD and SEC results, the channel-forming potency for all three analogues is reduced relative to [D-Leu^{10,12,14}]gA; the potency of [D-Ala^{10,12,14}] in fact is reduced by several orders of magnitude. The general agreement between the CD and SEC results and the reduced channel-forming potencies shows that the results are not significantly affected by the very different gramicidin:lipid ratios used in these different experiments (∼1:30 in the spectroscopic experiments and ∼10^{-6} in the single-channel experiments).

Hybrid Channel Experiments. The results in Figure 7 show that each analogue forms only one type of channel, but the structural identity of the channels is indeterminate on the basis of the homodimer experiments alone—except that that channels are SS dimers, based on their lifetimes. In view of the heterogeneity of conformations seen in the CD spectra and SEC chromatograms, we sought to identify more definitively the structure of the conducting analogue channels through heterodimer experiments, in which we examine whether a given analogue can form conducting heterodimers (hybrid channels) with structurally well-defined reference gramicidins (cf. refs *13*, *56*, and *57*). If a given analogue can form heterodimeric channels with a given reference analogue (e.g. [D-Leu^{10,12,14}]gA), then it must be able to form (SS) monomers that are structurally equivalent to the reference monomers (see ref *57* for a more detailed description of the experimental logic).

Figure 8 shows the results of such an experiment with [Ile^{10,12,14}]gA$^-$ and the reference [Leu^{10,12,14}]gA$^-$ (*31*). When either [Ile^{10,12,14}]gA$^-$ or [Leu^{10,12,14}]gA$^-$ is added by itself to both sides of a bilayer, we observe only a single well-defined channel type, which represents symmetric [Ile^{10,12,14}]gA$^-$ or [Leu^{10,12,14}]gA$^-$ homodimers (cf. Figure 7). No (symmetrical) channels are seen when either [Ile^{10,12,14}]gA$^-$ or [Leu^{10,12,14}]gA$^-$ is added asymmetrically, to only one side of a bilayer (see below). When both [Ile^{10,12,14}]gA$^-$ and [Leu^{10,12,14}]gA$^-$ are added symmetrically, to both sides of a bilayer, we observe channel events with current transition amplitudes similar to those seen with either of the two gramicidins by themselves. Similar results were recorded with [D-Val^{10,12,14}]gA and [Leu^{10,12,14}]gA.

These results could suggest that the subunit structures differ, such that only homodimeric channels will form. That is not the case, however. When [Ile^{10,12,14}]gA$^-$ and [Leu^{10,12,14}]-gA$^-$ are added to opposite sides of a bilayer, [Leu^{10,12,14}]gA$^-$ to one side and [Ile^{10,12,14}]gA$^-$ to the other, one does indeed observe channel activity (Figure 8)! When the [Leu^{10,12,14}]-gA$^-$-containing side is positive, one observes only one channel type and the amplitude of the current transitions is similar to that for symmetric [Leu^{10,12,14}]gA$^-$ channels. Conversely, when the [Ile^{10,12,14}]gA$^-$-containing side is positive, the amplitude of the current transitions is similar to that for symmetric [Ile^{10,12,14}]gA$^-$ channels. The presence of only one population of current transition amplitudes shows, again, that the channels form only when monomers are present on both sides of the bilayer. The orientation dependence of the current transition amplitudes is similar to that observed with Trp-substituted gramicidin channels (*23*) and shows that the Leu → Val substitutions at positions 10, 12, and 14 primarily affect ion entry. A similar conclusion was reached when the experiments were done with either [D-Val^{10,12,14}]gA or [D-Ala^{10,12,14}]gA and native [D-Leu^{10,12,14}]-gA as the reference. Table 2B summarizes the results.

That hybrid channels are able to form shows that the chemically different subunits are compatible and have similar backbone folding patterns and helix sense (*13*, *31*, *57*). Specifically, the conducting [Ile^{10,12,14}]gA$^-$ channels are dimers of LH, SS $\beta^{6.3}$-helical monomers, and the [D-Ala^{10,12,14}]-

gA and [D-Val^{10,12,14}]gA channels are formed by RH helices. It is in this context also important that the hybrid channel lifetimes are intermediate between those of the two symmetric parent channels, which shows that there is no strain at the junction between the two monomers. That is, any perturbation of the peptide backbone, or the amino side chains, induced by the Leu → Ile, Val, or Ala substitutions is local (and toward the C-terminal).

DISCUSSION

The structural and functional significance of the interfacial localization of aromatic amino acid residues in integral membrane proteins remains unclear—except for selected examples, such as the gramicidin channels, where it is established that the four Trps on each subunit are important for structure and function (*6*, *7*, *15*, *16*, *19*, *22*, *23*, *26*). Given the importance of the Trp residues, remarkably little is known about the structural and functional role of the residues adjacent to the Trps. In present experiments, therefore, neither the Trp residues nor their sequence positions were altered. Only the Leu residues next to the Trps have been changed semiconservatively to Ala, Val, or Ile. These aliphatic sequence changes have, perhaps surprisingly, large effects on channel structure and function. We will discuss the influence of the "spacers" on structure and structural heterogeneity and on channel function and then will summarize briefly the role of Trp and the adjacent residues in gramicidin channels.

Influence on Structure. The gramicidins display an intrinsic conformational heterogeneity (*58*, *59*). [D-Leu^{10,12,14}]gA, for example, adopts a number of predominantly DS β-helical conformations in ethanol (*45*) and dioxane (*59*) and unstructured monomeric conformations in dimethyl sulfoxide (*60*). As many as seven different conformers can be observed in a given solvent system. In lipid bilayers, or micelles that mimic a bilayer environment, [D-Leu^{10,12,14}]gA occurs primarily as a SS $\beta^{6.3}$-helical dimer, which corresponds to the transmembrane channel (*47*, *61*, *62*). The SS channel conformation of [D-Leu^{10,12,14}]gA is RH (*39*, *63*) and never LH (*31*). Even in bilayers there may be conformational heterogeneity, as [D-Leu^{10,12,14}]gA initially may form $\pi\pi^{5.6}$ DS structures in vesicles formed by phospholipids with polyunsaturated acyl chains (*64*, *65*). These DS conformers are metastable and do not function as ion conducting channels (*55*). In any given environment, the gramicidins therefore may occur as a mixture of conformers. The number of available conformations, the relative amount of each conformer that is present, and the kinetics of their interconversions (*15*, *16*) depend critically upon the chemical identity of the solvent or the membrane-forming lipids around the gramicidin molecules.

With triple substitutions of Leu^{10,12,14} in gA, the mix of conformers changes, regardless of the environment or the chosen experimental method. Whether examined in MeOH, EtOH, DMPC vesicles, or SDS micelles, the CD spectra of the analogues differ from that of gA (Figures 2-4), indicating that there has been a redistribution among the conformers. As might be expected from the structure of the substituted side chains, the CD spectra show characteristic differences between [Ile^{10,12,14}]gA$^-$ and [D-Val^{10,12,14}]gA on one hand and [D-Ala^{10,12,14}]gA on the other. Consistent with these observations, all of the SEC elution profiles (Figures 5 and 6) show increased proportions of DS conformations for the Ile^{10,12,14} and Val^{10,12,14} analogues and increased aggregation of the Ala^{10,12,14} analogue. The conformational susceptibility therefore is, in part, an intrinsic property of the particular amino acid sequence: each sequence exhibits a characteristic mix of conformations, the detailed characteristics of which also depend on the particular environment.

Two observations pertain to the channel conformation seen with D-Leu^{10,12,14}-substituted gramicidins. First, the CD and SEC results in DMPC are entirely consistent with all of the analogues (even the Ala-substituted analogue) having a significant fraction of molecules in a $\beta^{6.3}$ SS RH conformation. Second, the single-channel results, especially the heterodimer formation experiments, show that the channel conformation adopted by each of the analogues is very similar to that adopted by gA, with respect to both the backbone and the Trp side chain average orientations. The evidence for backbone structural similarity comes from the properties of the hybrid channels that form between gA and a reference analogue (Figure 8, Table 2). That hybrid channels can be formed by chemically dissimilar subunits means that the backbone folding patterns are compatible and specifically of the same helix sense (*14*, *31*). Furthermore, the observations that the hybrid channel conductances and average lifetimes are comparable to those of the symmetric parent channels (Table 2) argue that there is little or no energetic cost associated with the formation of the hydrogen bond-stabilized heterodimer (cf. refs *13* and *66*). Unfortunately, it was not possible to quantify the relative heterodimer formation rates because of the overlapping homodimer and heterodimer peaks (Figures 7 and 8). The individual subunit backbones therefore are folded similarly to each other. The evidence for Trp side chain structural similarity comes from the single-channel conductance results (below).

Influence on Channel Function. The results illustrate the difficulties one may encounter in structure−function studies. For all four gramicidins, there is a single functionally active conformation, the RH, SS $\beta^{6.3}$-helical dimer; but the three D-Leu^{10,12,14}-substituted analogues occur as several conformers—even in a phospholipid environment. Some of these conformers are DS structures, most likely an inert $\pi\pi^{5.6}$ DS dimer. This divergence means that one cannot necessarily in a straightforward manner correlate spectroscopic measurements, which are biased toward the predominant conformer (and usually are done at relatively high concentrations), and functional measurements, which may sample only a small fraction of the molecular species (and usually are done at very low concentrations).

Effects on Single-Channel Conductance. Triple substitutions of D-Leu^{10,12,14} in gA cause an approximate 25% decrease in the Cs^+ conductance, regardless of whether the newly introduced amino acids are Ala, Val, or Ile (Table 2). Comparable conductance changes can be caused by only a single Trp → Phe substitution (Table 2; see also ref *7*). We draw three inferences from these results. First, because the Trp side chain dipoles are important for promoting the channels' cation conductance (*7*, *12*, *22*, *26*), the Trp indole ring orientations, though altered, cannot be changed much from those of [D-Leu^{10,12,14}]gA channels for any of the analogues; i.e., each of the position-10, -12, and -14

analogues retains indole dipole orientations that are close enough to the native orientations to yield 75% of the gA Cs^+ conductance. Second, there is no increase in the dispersity of single-channel currents when residues 10, 12, and 14 are substituted. Third, whatever the packing of the Leu spacer residues, they support (nearly) optimum Trp indole ring orientations for cation permeation, which suggests that the Trp orientation is determined largely by the properties of the indole ring itself as it adjusts to the polarity profile at the solution interface. Whether steric crowding is reduced, by making the Leu side chains smaller, or increased, by introducing branching at the β-carbons, the cation conductance decreases. One should not overinterpret the results, however. The quantitative similarities among the cation conductances of the analogue channels could result from fortuitous canceling (or summing) of different distinct effects on the four Trp residues as the intervening residues at 10, 12, and 14 are changed. Further experiments with singly substituted analogues would be needed to clarify this issue.

Effects on Average Channel Lifetime. When Leu 10, 12, and 14 are replaced, the lifetimes of the (SS) analogue channels decrease. Moreover, DS conformations appear in the population of conformations within membranes (whereas under equilibrium conditions DS conformations are almost nonexistent for gA in DMPC or DPhPC bilayers). When Ile or Val occupy positions 10, 12, and 14, the average channel lifetime is reduced about 50%, and DS conformations comprise about half of the molecular population (as evidenced by the SEC data). For [D-Ala^{10,12,14}]gA the effects are even more dramatic: The channel lifetime is reduced by 85−90% compared to gA channels, and aggregates of higher order than dimer appear in the population. This correlation could suggest that the increased conformational heterogeneity may be related to the decreased channel lifetime. Specifically, the reduced lifetimes (and decreased channel-forming potencies) show that the analogue (SS) membrane-spanning channels are less stable than the parent [D-Leu^{10,12,14}]gA channels. The decreased stability means that other, normally less favored conformers, will be relatively abundant. The higher order aggregates seen with [D-Ala^{10,12,14}]-gA, however, could arise because the less bulky alanines permit stronger interactions between the aromatic side chains (and/or the backbones) in adjacent gramicidins.

Perspective on Tryptophans and Spacer Residues. Numerous experiments have shown the importance of Trp 9, 11, 13, and 15 for gramicidin channel structure and function. These Trp residues tend to anchor each gA monomer within the lipid monolayer leaflet to which it is added (*6*), the Trps drive the folding of gA into the SS channel conformation in lipids (*15*, *16*, *67*, *68*), and the Trp dipoles promote the flux of cations through the channel (*7*, *12*, *22*, *26*). It also has been proposed that changes in Trp orientations could account for the appearance of channels having conductances that differ from those of the "standard" channels (*69*). The present results suggest that this cannot be the case, because there were no significant changes in the distribution of current transition amplitudes, as compared to [D-Leu^{10,12,14}]gA (*43*), whether the volume of the "spacer" residues is reduced ([D-Ala^{10,12,14}]gA) or increased at the β-carbon ([D-Val^{10,12,14}]gA and [Ile^{10,12,14}]gA$^-$); see Figure 7. Notwithstanding, the results presented in this paper show that the Trp functions are modulated by the intervening "spacer" residues at positions 10, 12, and 14 and by changes in backbone dynamics brought about by the substitutions. Substituting the γ-branched Leu by the β-branched Val or Ile would be expected to make the make the backbone more rigid, which may account for the effects on ion entry (e.g. Figure 8). The net effects therefore are due to rather complex interplay between Trp residues, aliphatic side chains, lipid/solvent molecules, and backbone folding. The combined effects of these interactions present a challenge for molecular modeling.

REFERENCES

1. Michel, H., and Deisenhofer, J. (1990) *Curr. Top. Membr. Transp. 36*, 53−69.
2. Weiss, M., Abele, U., Weckesser, J., Welte, W., Schiltz, E., and Schulz, G. E. (1991) *Science 254*, 1627−1630.
3. Schiffer, M., Chang, C. H., and Stevens, F. J. (1992) *Protein Eng. 5*, 213−214.
4. Wimley, W. C., and White, S. H. (1993) *Biochemistry 32*, 6307−6312.
5. Doyle, D. A., Cabral, J. M., Pfuetzner, R. A., Kuo, A., Gulbis, J. M., Cohen, S. L., Chait, B. T., and MacKinnon, R. (1998) *Science 280*, 69−77.
6. O'Connell, A. M., Koeppe, R. E., II, and Andersen, O. S. (1990) *Science 250*, 1256−1259.
7. Becker, M. D., Greathouse, D. V., Koeppe, R. E., II, and Andersen, O. S. (1991) *Biochemistry 30*, 8830−8839.
8. Hu, W., Lee, K. C., and Cross, T. A. (1993) *Biochemistry 32*, 7035−7047.
9. Ketchem, R. R., Hu, W., and Cross, T. A. (1993) *Science 261*, 1457−1460.
10. Koeppe, R. E., II, Killian, J. A., and Greathouse, D. V. (1994) *Biophys. J. 66*, 14−24.
11. Hu, W., Lazo, N. D., and Cross, T. A. (1995) *Biochemistry 34*, 14138−14146.
12. Hu, W., and Cross, T. A. (1995) *Biochemistry 34*, 14147−14155.
13. Durkin, J. T., Koeppe, R. E., II, and Andersen, O. S. (1990) *J. Mol. Biol. 211*, 221−234.
14. Durkin, J. T., Providence, L. L., Koeppe, R. E., II, and Andersen, O. S. (1992) *Biophys. J. 62*, 145−159.
15. Salom, D., Bañó, M. C., Braco, L., and Abad, C. (1995) *Biochem. Biophys. Res. Commun. 209*, 466−473.
16. Salom, D., Pérez-payá, E., Pascal, J., and Abad, C. (1998) *Biochemistry 37*, 14279−14291.
17. Bamberg, E., Noda, K., Gross, E., and Läuger, P. (1976) *Biochim. Biophys. Acta 419*, 223−228.
18. Tredgold, R. H., and Hole, P. N. (1976) *Biochim. Biophys. Acta 443*, 137−142.
19. Heitz, F., Spach, G., and Trudelle, Y. (1982) *Biophys. J. 40*, 87−89.
20. Mazet, J. L., Andersen, O. S., and Koeppe, R. E., II. (1984) *Biophys. J. 45*, 263−276.
21. Sawyer, D. B., Williams, L. P., Whaley, W. L., Koeppe, R. E., II, and Andersen, O. S. (1990) *Biophys. J. 58*, 1207−1212.
22. Becker, M. D., Koeppe, R. E., II, and Andersen, O. S. (1992) *Biophys J. 62*, 25−27.
23. Fonseca, V., Daumas, P., Ranjalahy-Rasoloarijao, L., Heitz, F., Lazaro, R., Trudelle, Y., and Andersen, O. S. (1992) *Biochemistry 31*, 5340−5350.
24. Seoh, S.-A., and Busath, D. (1995) *Biophys. J. 68*, 2271−2279.
25. Koeppe, R. E., II, Vogt, T. C. B., Greathouse, D. V., Killian, J. A., and De-Kruijff, B. (1996) *Biochemistry 35*, 3641−3648.
26. Andersen, O. S., Greathouse, D. V., Providence, L. L., Becker, M. D., and Koeppe, R. E., II. (1998) *J. Am. Chem. Soc. 120*, 5142−5146.
27. Weiss, L. B., and Koeppe, R. E., II. (1985) *Int. J. Pept. Protein Res. 26*, 305−310.
28. Mattice, G. L., Koeppe, R. E., II, Providence, L. L., and Andersen, O. S. (1995) *Biochemistry 34*, 6827−6837.
29. Greathouse, D. V., Hinton, J. F., Kim, K. S., and Koeppe, R. E., II. (1994) *Biochemistry 33*, 4291−4299.

30. Stewart, J. M., and Young, J. D. (1984) *Peptide Synthesis*; Pierce Chemical Co., Rockford, IL.
31. Koeppe, R. E., II, Providence, L. L., Greathouse, D. V., Heitz, F., Trudelle, Y., Purdie, N., and Andersen, O. S. (1992) *Proteins 12*, 49−62.
32. Providence, L. L., Andersen, O. S., Greathouse, D. V., Koeppe, R. E., II, and Bittman, R. (1995) *Biochemistry 34*, 16404−16411.
33. Turner, G. L., Hinton, J. F., Koeppe, R. E., II, Parli, J. A., and Millett, F. S. (1983) *Biochim. Biophys. Acta 756*, 133−137.
34. Mobashery, N., Nielsen, C., and Andersen, O. S. (1997) *FEBS Lett. 412*, 15−20.
35. Killian, J. A. (1992) *Biochim. Biophys. Acta 1113*, 391−425.
36. He, K., Ludtke, S. J., Wu, Y., and Huang, H. W. (1993) *Biophys. J. 64*, 157−162.
37. He, K., Ludtke, S. J., Wu, Y., Huang, H. W., Andersen, O. S., Greathouse, D., and Koeppe, R. E., II (1994) *Biophys. Chem. 49*, 83−89.
38. Lee, K. C., Hu, W., and Cross, T. A. (1993) *Biophys. J. 65*, 1162−1167.
39. Arseniev, A. S., Barsukov, I. L., Bystrov, V. F., Lomize, A. L., and Ovchinnikov, Yu. A. (1985) *FEBS Lett. 186*, 168−174.
40. Wallace, B. A. (1987) in *Ion Transport Through Membranes* (Yagi, K., and Pullman, B., Eds.) pp 255−275, Academic Press, Tokyo.
41. Bañó, M. C., Braco, L., and Abad, C. (1988) *J. Chromatogr. 458*, 105−116.
42. Andersen, O. S. (1983) *Biophys. J. 41*, 119−133.
43. Sawyer, D. B., Koeppe, R. E., II, and Andersen, O. S. (1989) *Biochemistry 28*, 6571−6583.
44. Wallace, B. A. (1986) *Biophys. J. 49*, 295−306.
45. Veatch, W. R., Fossel, E. T., and Blout, E. R. (1974) *Biochemistry 13*, 5249−56.
46. Masotti, L., Spisni, A., and Urry, D. W. (1980) *Cell Biophys. 2*, 241−254.
47. Wallace, B. A., Veatch, W. R., and Blout, E. R. (1981) *Biochemistry 20*, 5754−5760.
48. Veatch, W. R. (1973) Gramicidin A-Conformations and Aggregation, Ph.D. Thesis, Harvard University.
49. Koeppe, R. E., II, Hodgson, K. O., and Stryer, L. (1978) *J. Mol. Biol. 121*, 41−54.
50. Koeppe, R. E., II, Berg, J. M., Hodgson, K. O., and Stryer, L. (1979) *Nature 279*, 723−725.
51. Arseniev, A. S., Barsukov, I. L., and Bystrov, V. F. (1985) *FEBS Lett. 180*, 33−39.
52. Langs, D. A. (1988) *Science 241*, 188−191.
53. Langs, D. A., Smith, G. D., Courseille, C., Precigoux, G., and Hospital, M. (1991) *Proc. Natl. Acad. Sci. U.S.A. 88*, 5345−5349.
54. Bañó, M. C., Braco, L., and Abad, C. (1989) *FEBS Lett. 250*, 67−71.
55. Girshman, J., Greathouse, D. V., Koeppe, R. E., II, and Andersen, O. S. (1997) *Biophys. J. 73*, 1310−1319.
56. Veatch, W., and Stryer, L. (1977) *J. Mol. Biol. 113*, 89−102.
57. Andersen, O. S., Saberwal, G., Greathouse, D. V., and Koeppe, R. E., II. (1996) *Indian J. Biochem. Biophys. 33*, 331−342.
58. Bystrov, V. F., and Arseniev, A. S. (1988) *Tetrahedron 44*, 925−940.
59. Abdul-Manan, Z., and Hinton, J. F. (1994) *Biochemistry 33*, 6773−6783.
60. Roux, B., Brueschweiler, R., and Ernst, R. R. (1990) *Eur. J. Biochem. 194*, 57−60.
61. Urry, D. W. (1971) *Proc. Natl. Acad. Sci. U.S.A. 68*, 672−676.
62. Weinstein, S., Wallace, B. A., Blout, E. R., Morrow, J. S., and Veatch, W. R. (1979) *Proc. Natl. Acad. Sci.; U.S.A. 76*, 4230−4234.
63. Nicholson, L. K., and Cross, T. A. (1989) *Biochemistry 28*, 9379−9385.
64. Cox, K. J., Ho, C., Lombardi, J. V., and Stubbs, C. D. (1992) *Biochemistry. 31*, 1112−1117.
65. Sychev, S. V., Barsukov, L. I., and Ivanov, V. T. (1993) *Eur. Biophys. J. 22*, 279−288.
66. Durkin, J. T., Providence, L. L., Koeppe, R. E., II, and Andersen, O. S. (1993) *J. Mol. Biol. 231*, 1102−1121.
67. Cotten, M., Xu, F., and Cross, T. A. (1997) *Biophys. J. 73*, 614−623.
68. Ketchem, R., Roux, B., and Cross, T. (1997) *Structure 5*, 1655−1669.
69. Prasad, K. U., Trapane, T. L., Busath, D., Szabo, G., and Urry, D. W. (1983) *Int. J. Pept. Protein Res. 22*, 341−347.
70. Arseniev, A. S., Lomize, A. L., Barsukov, I. L., and Bystrov, V. F. (1986) *Biol. Membr. 3*, 1077−1104.
71. Killian, J. A., Taylor, M. J., and Koeppe, R. E., II. (1992) *Biochemistry 31*, 11283−11290.

BI982043M